Brain Research 1857 (2025) 149616

Contents lists available at ScienceDirect

Brain Research

journal homepage: www.elsevier.com/locate/brainres

Research paper

From encoding to recognition: Exploring the shared neural signatures of visual memory

Berfin Ozdemir, Géza Gergely Ambrus *,[1]

Department of Psychology, Bournemouth University, Poole House, Talbot Campus, Fern Barrow, Poole, Dorset BH12 5BB, United Kingdom

ARTICLE INFO

Keywords:
Multivariate pattern analysis
EEG
Memory
Learning
Encoding
Recollection
Recognition

ABSTRACT

This study investigated the shared neural dynamics underlying encoding and recognition processes across diverse visual object stimulus types in short term experimental familiarization, using EEG-based representational similarity analysis and multivariate cross-classification. Building upon previous research, we extended our exploration to the encoding phase. We show early visual stimulus category effects around 150 ms post-stimulus onset and old/new effects around 400 to 600 ms. Notably, a divergence in neural responses for encoding, old, and new stimuli emerged around 300 ms, with items encountered during the study phase showing the highest differentiation from old items during the test phase. Cross-category classification demonstrated discernible memory-related effects as early as 150 ms. Anterior regions of interest, particularly in the right hemisphere, did not exhibit differentiation between experimental phases or between study and new items, hinting at similar processing for items first encountered, irrespective of experiment phase. While short-term experimental familiarity did not consistently adhere to the old >new pattern observed in long-term personal familiarity, statistically significant effects are observed specifically for experimentally familiarized faces, suggesting a potential unique phenomenon specific to facial stimuli. Further investigation is warranted to elucidate underlying mechanisms and determine the extent of face-specific effects. Lastly, our findings underscore the utility of multivariate cross-classification and cross-dataset classification as promising tools for probing abstraction and shared neural signatures of cognitive processing.

1. Introduction

Research has shown that memory-related processing unfolds over time (Staresina & Wimber, 2019), with distinct stages characterized by unique patterns of neural activity (Ambrus, 2024; Dalski et al., 2022a). Early in the processing stream, sensory stimuli elicit rapid neural differentiation, leading to the encoding of stimulus characteristics. Research using electroencephalography (EEG) and magnetoencephalography (MEG) has revealed rapid discrimination and classification of visual stimuli, such as human faces, buildings, animals, and objects, occurring as early as the P1-N1-N170 range (Carlson et al., 2013; Klink et al., 2023; Xie et al., 2022). Subsequently, memory-related processes become prominent, as information is recalled and/or stored for later retrieval. The transition of neural signals from stimulus-driven representations to memory-related processing is a critical period that marks the shift from perceptual analysis to higher-order cognitive functions associated with memory formation and recollection.

The objective of this study is to provide a data-driven investigation of the temporal neural dynamics involved in the cognitive processing associated with the encoding of novel stimuli, later recognizing studied items as old, and distinguishing novel items as new, shared across participants and visual stimulus types.

Subsequent Memory Effects. Event-related potential studies that investigate both study and recall primarily focus on subsequent memory effects (SME), that is, the neural patterns or activity differences between items that are later remembered versus those that are later forgotten (Mecklinger & Kamp, 2023). These effects are typically identified by comparing the brain activity associated with stimuli that participants later recall or recognize correctly in memory tests with brain activity linked to stimuli that participants later fail to recall or recognize. Subsequent memory effects are characterized by distinct components, including early frontal SMEs (ca. 300 and 600 ms) theorized to indicate of semantic processing (Otten & Rugg, 2001), early parietal SMEs (350 and 500 ms) thought to be associated with feature binding (Meßmer

---

* Corresponding author.
E-mail address: g.ambrus@gmail.com (G.G. Ambrus).

[1] 0000-0002-8400-8178.

https://doi.org/10.1016/j.brainres.2025.149616
Received 12 January 2025; Received in revised form 24 March 2025; Accepted 3 April 2025

et al., 2021), and sustained late frontal SMEs (ca. 550 ms post-stimulus) reflecting elaborative encoding (Kamp & Zimmer, 2015). These components interact with preparatory mechanisms, influencing memory performance even before stimulus presentation (pre-stimulus SME, (Yick et al., 2016)). Moreover, SMEs can be modulated by various factors such as encoding tasks, the content of information, distinctiveness, as well as external factors. In sum, these effects are thought to capture the neural signatures associated with successful memory formation and recognition, highlighting the brain regions or activity patterns that contribute to memory performance.

Old/new effects. In recognition memory tasks, ERPs reveal a greater positivity for correctly identified studied ("old") items compared to correctly rejected unstudied ("new") items. This mid-frontal old/new effect, often referred to as the FN400, emerges around 300 ms post-stimulus, peaking at approximately 500 ms before declining, typically over frontal scalp locations. This effect is associated with familiarity, which refers to the undifferentiated experience of "just knowing" that something was previously encountered, without retrieval of contextual information (Yonelinas, 2002). In contrast, the parietal ERP old/new effect, known as the late positive component (LPC), emerges later, between 500–800 ms post-stimulus onset, peaking over the left or central parietal scalp channels. This parietal effect is linked with recollection, which involves a detailed and often vivid experience of "reliving the past", entailing the recovery of episodic information such as where and when the original encounter occurred. These old/new effects have been found to exhibit distinct process-selectivity and temporal structure (Kwon et al., 2023).

Functional neuroanatomy. The insights gained from EEG studies into the temporal dynamics of neural activity are complemented by the functional neuroanatomy of memory processes. The Hippocampal Indexing Theory (Teyler & Rudy, 2007) and the Complementary Learning Systems (O'Reilly & Norman, 2002) frameworks assign distinct roles to the hippocampus and neocortex in memory processing. During encoding, sensory information from various modalities is processed by different areas of the neocortex. These patterns of neocortical activations are condensed and transmitted to the hippocampus via the entorhinal cortex. Within the hippocampal formation, particularly in the dentate gyrus, these patterns undergo pattern separation, a process that ensures distinct representations are formed for similar inputs (Yassa & Stark, 2011). These representations are then bound together and indexed in the hippocampal CA3, strengthening connections between neurons representing the elements of the memory. During retrieval, cues or features of a memory trigger activation in the hippocampus. Specifically, when a feature of the original stimulus is present, in a process referred to as pattern completion (Horner et al., 2015), CA1, in tandem with CA3, mediates the reactivation of the appropriate cortical areas associated with the memory. Activation of these cortical areas allows for the re-experiencing of the event as a memory, as the cortical representation of the original experience is reinstated. This hippocampus-to-neocortex cascade of memory reinstatement occurs ca. 500 to 1500 ms following the cue (Staresina & Wimber, 2019).

Encoding/retrieval state studies. Earlier models, such as the Hemispheric Encoding and Retrieval Asymmetry (HERA) model (Tulving et al., 1994) proposed differential involvement of the left and right prefrontal cortices during episodic memory processes. According to HERA, the left prefrontal cortex (PFC) primarily participates in encoding, while the right PFC is predominantly engaged in retrieval. Although evidence supporting this model spans various stimulus types, it remains subject to interpretation and debate (Andreau & Torres Batán, 2019; Kelley et al., 1998; Rossi et al., 2011; Wagner et al., 1998). More recent studies aimed to unravel the neural mechanisms underlying memory encoding and retrieval processes amidst overlapping or interfering events from the past and present. Richter et al. (2016) utilized fMRI decoding analyses to explore how the hippocampal memory system manages encoding and retrieval states, finding distinct contributions of the medial prefrontal cortex and hippocampus to these processes, with the hippocampus signaling the tradeoff between encoding and retrieval and the medial prefrontal cortex representing past experiences in relation to new learning. Smith et al. (2022) investigated the impact of temporal overlap between present and past events on memory processing using EEG, revealing a bias towards retrieval with increased temporal overlap, impairing memory for the past event when encoding the present event was the goal. Long & Kuhl (2019) demonstrated that biases towards encoding or retrieval states can be decoded from spectral EEG patterns, predicting later memory performance for overlapping events. Hong et al. (2023) investigated EEG microstates during mnemonic tasks biased towards encoding or retrieval, revealing sustained differences in engagement of Microstate E between encoding and retrieval, highlighting the relationship between cortical networks, the hippocampus, and temporal factors in memory processing. Finally, in their study on episodic memory using intracranial recordings, Mohan et al. (2024) observed traveling waves propagating in posterior-to-anterior and anterior-to-posterior directions during encoding and retrieval phases, respectively.

While ERP analyses are invaluable for characterizing stimulus-specific (Bentin et al., 1996; Bötzel & Grüsser, 1989; Tanaka et al., 2009; Watanabe et al., 2003; Yildirim-Keles et al., 2025) and memory-related (Curran, 1999; Danker et al., 2008; Kwon et al., 2023; Mecklinger & Kamp, 2023; Wolk et al., 2006, Wolk et al., 2009) neural responses, multivariate approaches capture distributed patterns that are not reducible to time-locked averages. This is particularly advantageous for cross-classification, as it allows for the identification of shared neural representations across stimulus types and participants. As seen, research has extensively explored the multifaceted nature of the neural correlates of various memory functions. The distinct temporal dynamics of encoding and recall processes, however, have yet to be fully characterized.

The present study. In a study by Ambrus (Ambrus, 2024), multivariate cross-dataset classification analysis was employed to explore the common neural signatures underlying recognition memory across various stimulus types and experimental conditions. Cross-dataset classification from familiar and remembered objects revealed an early-late dissociation: shared recognition signals were observed only in the later, post-400 ms window for correctly remembered objects, whereas successful cross-decoding for familiar objects was evident in the early, ca. 200 ms period as well. The study also showcased the potential of cross-classification to investigate general, participant- and stimulus-independent neural signatures of memory processes. Subsequently, in Klink and colleagues (2023) we confirmed the generalizability of neural signals for familiar and unfamiliar faces and scenes using cross-participant and cross-category classification within one experiment.

Aims. Building on the results and methods of these studies, the aims of this present investigation were the following. Firstly, we sought to replicate general neural signatures of recognition by investigating short-term memory processes across diverse sets of stimuli within one experiment. By contrasting neural responses to old and new items during a memory task, we aimed to identify consistent patterns indicative of recognition across various stimulus types. More importantly, we aimed to extend our investigation to the encoding phase, probing neural signatures associated with the initial encoding of stimuli into memory. Here, we aimed to uncover common patterns that differentiate memory formation and recall across different types of stimuli. In sum, we sought to characterize the neural dynamics underlying both recognition and encoding processes, elucidating the temporal evolution and spatial distribution of neural activity associated with memory-related processing.

2. Methods

2.1. Participants

Data from 22 volunteers were included in the study. The sample consisted of 5 male and 17 female participants with a mean age of 21.36

years (SD = 2.61). This sample size is comparable to that of similar studies employing multivariate cross-classification and cross-dataset classification techniques (Dalski et al., 2022b; Dalski et al., 2022a; Li et al., 2022). Participants were students and employees of Bournemouth University and were recruited through the SONA research participation system and received partial course credits or volunteered their time without compensation. All participants reported being right-handed and having normal or corrected-to-normal vision. Participants reported no history of neurological conditions or CNS-active medication use at the time of the study. All participants provided written informed consent, and the study was approved by the Bournemouth University Research Ethics committee [no. 49206]. The study was conducted in accordance with the Declaration of Helsinki.

2.2. *Experimental design*

Stimuli. Stimuli consisted of color images drawn from eight stimulus types: faces, bodies, toys, houses; animals, plants, vehicles, furniture. Faces included unfamiliar younger and older male and female faces, generated using the https://generated.photos/anonymizer website. The rest of the stimuli were collected from various internet sources (mainly Wikimedia Commons). Body stimuli were images of male and female athletes from various countries with the head area erased. Toy stimuli included various objects designed for play or enjoyment. House stimuli were images of one to three-story residential structures. Animal stimuli included photographs of land and sea animals. Plant stimuli consisted of images of fruits and vegetables. Vehicle stimuli comprised of photographs depicting machinery used for transportation on land and water. Furniture stimuli included household articles and domestic furnishings commonly found in residential settings. The background of each image was removed, and stimuli were resized to 350 × 350 pixels. For stimuli examples, see Fig. 1**D**.

Study blocks. In each study block (see Fig. 1**B**), participants viewed 16 images randomly selected from four stimulus categories (4 items from each). The stimuli were displayed centrally on a grey background for 1000 ms each. Participants were tasked with memorizing the presented items. After every eight trials, participants took a self-paced break.

Test blocks. During each test block (see Fig. 1**C**), participants were presented with a total of 32 stimuli, comprising 16 previously presented items and 16 novel stimuli (balanced across stimulus types). These were presented in a random order and displayed for 1000 ms each. Participants were instructed to determine whether each stimulus was old or new, indicating whether it had been seen in the preceding study phase or not. Additionally, participants provided a confidence rating for each decision, ranging from “guess” to “moderately confident” to “highly confident”; this factor is not analyzed in this report. Participants did not receive feedback on their performance during the experiment.

The study and test blocks were repeated four times, with an average time difference of approximately two minutes between the presentation of an item for study and recall (mean and SD: 113.26 ± 4.82 s, calculated post-data collection). Note that the study and test items were randomly assigned for each participant. Throughout the experiment, participants studied a total of 128 items, 16 within a single stimulus category, resulting in a total of 2816 study trials across all participants. Each study item was subsequently presented during the test phase alongside an equal number of novel stimuli from the same stimulus set, resulting in 384 trials per participant. The overall correct response rate was 88.31 %, with all participants providing correct responses on 4974 test trials (hits: 2500, correct rejections: 2474, misses: 316, false alarms: 342).

The experiment included two additional test tasks involving items that were either pre-experimentally familiar or unfamiliar. One task featured famous and unknown faces and buildings, while the other included interior and exterior scenes depicting the university campus and images of unfamiliar scenes from elsewhere. These tasks exclusively consisted of test blocks without any study phases. The findings from these tasks are not reported in this paper. The sequence of tasks was the same for all participants and followed a predetermined order: 0) a brief practice session, 1) pre-experimentally familiar or unfamiliar faces and buildings, 2) experimentally familiarized faces, bodies, toys, and houses, 3) pre-experimentally familiar or unfamiliar campus scenes, 4) and experimentally familiarized animals, plants, vehicles, and furniture (see Fig. 1**A**).

2.3. *Electroencephalography*

EEG recordings were obtained using a 64-channel BioSemi ActiveTwo device, with a sampling rate of 1024 Hz. During the recordings, the distance between the participants’ eyes and the computer screen was set to 110 cm. Common-average referenced EEG signals were notch-filtered at 50 Hz and bandpass-filtered between 0.1 and 40 Hz. The data were then segmented from −200 to 1200 ms relative to stimulus onset and baseline-corrected using the first 200 ms as the reference period. Subsequently, the data were downsampled to a sampling rate of 200 Hz. No additional processing steps were applied to the data (Ambrus et al., 2021; Dalski et al., 2022b; Delorme, 2023; Grootswagers et al., 2017). The preprocessing pipeline was implemented using MNE-Python (Gramfort et al., 2013, Gramfort et al., 2014).

2.4. *Data analysis*

For the purposes of this report, leave-one-subject-out (LOSO) and leave-one-category-out classification schemes were employed. Linear Discrimination Analysis (LDA) classifiers, available in the scikit-learn Python package, were utilized for classification. Time-resolved representational similarity analyses, time-resolved classification, and searchlight analyses were conducted.

We focused exclusively on trials with correct answers, regardless of the participants’ response confidence levels. To ensure balanced class representation and to prevent biases that arise from imbalanced data, we under-sampled the trials. Specifically, we under-sampled the number of trials for each participant to match the minimum trial count across the classes of interest. This under-sampling procedure was applied during both classifier training and testing (for a similar approach see (Ambrus, 2024; Klink et al., 2023)).

2.4.1. *Leave-one-subject-out and cross-condition classification*

Understanding the abstraction and generalizability of neural signals is crucial for investigating the underlying mechanisms of cognition. These manifestations of complex cognitive processes may extend beyond specific conditions or stimuli, suggesting shared representations across diverse contexts. These shared representations offer insights into the fundamental principles underlying cognitive operations, providing a glimpse into the generalizable aspects of neural processing. In this study, we utilized cross-participant and cross-condition classification techniques to explore stimulus- and participant-independent patterns of memory encoding and recognition.

Cross-participant representational similarity analysis (Fig. 2) allowed us to examine the time-resolved representational structure shared across participants across all stimulus types. While this method facilitates the testing of complex models using model correlations, it is not well-suited for cross-stimulus classification. To address this, we employed cross-participant and cross-category classification analyses (Fig. 3), enabling us to investigate both participant-independent effects and the shared neural signals of mnemonic processes across stimulus categories. For a similar approach, see Ely and Ambrus (Ely & Ambrus, 2025).

In leave-one-subject-out (LOSO) classification, data from one participant is withheld as a test set, while the data from the remaining participants are used to train the classifier. This process is repeated for each participant in the dataset, ensuring that every participant

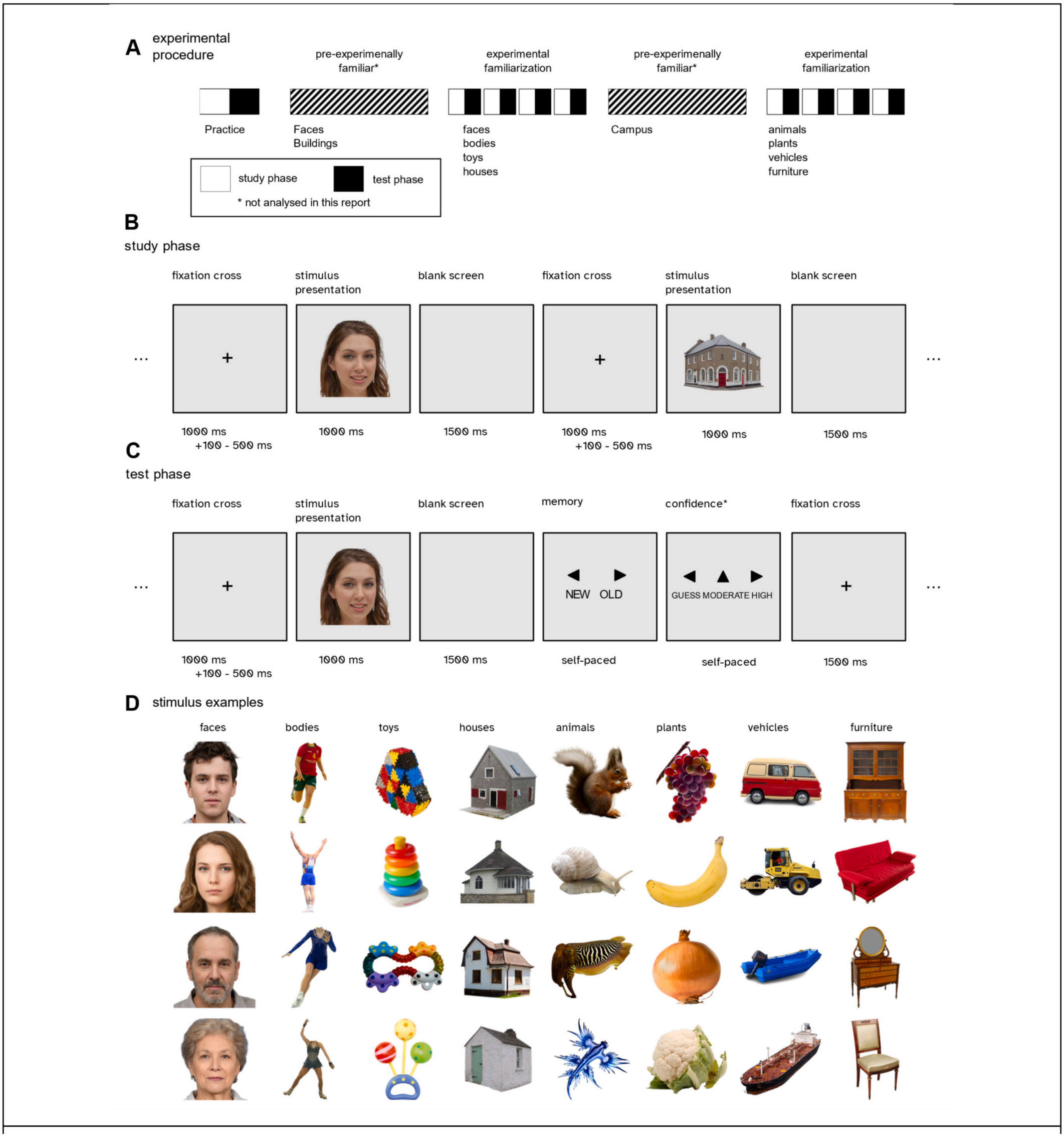

(caption on next page)

Fig. 1. Experimental design. The experiment included study and test phases (**A**). During the study phase (**B**), participants were instructed to memorize images from four stimulus types (faces, houses, toys, bodies, or animals, plants, vehicles, furniture), each presented for 1000 ms. In the subsequent test phase (**C**), study items were reintroduced alongside novel images, also presented for 1000 ms. Participants were prompted to make old/new decisions followed by confidence judgments (guess/moderate/high confidence). Note that two test-blocks with pre-experimentally familiar stimuli were also included (famous/unknown faces and buildings, familiar and unfamiliar scenes); analysis of the data from these blocks will be reported elsewhere. (**D**) Example stimuli in the eight stimulus categories.† †**Source of the example images: File**:20141206 1449 PORISR 6188.jpg. Wikimedia Commons. https://w.wiki/9MSD. File:European Championships 2022–08-18 Senior Men All-around competition Subdivision 2 (Norman Seibert) – DSC 3561.jpg. *Wikimedia Commons*. https://w.wiki/9MSF. File:2018 EC Anita Östlund 2018–01-20 21–39-46.jpg. *Wikimedia Commons*. https://w.wiki/9MSG. File:2018 EC Julia Sauter 2018–01-18 14–06-13 (4).jpg. *Wikimedia Commons*. https://w.wiki/9MSJ. File: WallEinZaks.jpg (Wikipedia, the free encyclopedia. https://en.wikipedia.org/wiki/File:WallEinZaks.jpg. File:Toys 2013–056-048 (12910779433).jpg. *Wikimedia Commons*. https://w.wiki/9MSL. File:Plastic baby rattle toy.jpg. *Wikimedia Commons*. https://w.wiki/9MSN. File:Sonajeros.jpg. *Wikimedia Commons*. https://w.wiki/9MSP. File:2009 Trip – Cape Breton Island (3940249474).jpg. *Wikimedia Commons*. https://w.wiki/9MSQ. File:Circular house – geograph.org.uk – 483214.jpg. *Wikimedia Commons*. https://w.wiki/9MSS. File:Újezd u Cerhovic, small house.jpg. *Wikimedia Commons*. https://w.wiki/9MST. File:Small house at Dullaghan – geograph.org.uk – 120249.jpg. *Wikimedia Commons*. https://w.wiki/9MSV. File:Squirrel posing.jpg. *Wikimedia Commons*. https://w.wiki/9MSW. File:Snail.jpg. *Wikimedia Commons*. https://w.wiki/9MSY. File:Cuttlefish zebra pattern.jpg. *Wikimedia Commons*. https://w.wiki/9MSa. File:Blue dragon-glaucus atlanticus (8599051974).jpg. *Wikimedia Commons*. https://w.wiki/9MSb. File:Pinot Grigio-20201027-RM-114053.jpg. *Wikimedia Commons*. https://w.wiki/9MSe. File:Banana-Single.jpg. *Wikimedia Commons*. https://w.wiki/9MSf. File:Onion on White.JPG. *Wikimedia Commons*. https://w.wiki/9MSg. File:Chou-fleur 02.jpg. *Wikimedia Commons*. https://w.wiki/9MTD. File:1990 s mini van in the street.jpg. *Wikimedia Commons*. https://w.wiki/9MSx. File:Road Roller 9925 (14660722798).jpg. *Wikimedia Commons*. https://w.wiki/9MSz. File:Oliver Dinghy Boat Yacht Tender- Oliverboat.jpg. *Wikimedia Commons*. https://w.wiki/9MT2. File:Mississippi Voyager 4.jpg. *Wikimedia Commons*. https://w.wiki/9MT3. File:American cupboard, c. 1790–1820, cherry and butternut, Dayton Art Institute.JPG. *Wikimedia Commons*. https://w.wiki/9MT4. File:Sofa Ligne Roset (fcm).jpg. *Wikimedia Commons*. https://w.wiki/9MT5. File: https://cdn2.picryl.com/photo/2018/11/11/dressing-chest-thomas-seymour-boston-c-1810-mahogany-birds-eye-maple-satinwood-385c58-1024.jpg *Pycril.com* public domain images. https://tinyurl.com/y4ru4ze2. File:Mahoniehouten rechte neo-Empire stoel, objectnr 8083–15.JPG. *Wikimedia Commons*. https://w.wiki/9MT6.

contributes to both the training and testing phases. Excluding each participant in turn from the training set, LOSO classification facilitates the exploration of general, participant-independent effects.

Cross-category classification involves training the classifier on data from one task or experimental condition and evaluating its performance on data from a different task or condition. This method, similar to multivariate cross-classification (Kaplan et al., 2015), enables the examination of the classifier's generalization capabilities across distinct tasks or conditions. Assessing whether the learned patterns or features are specific to particular contexts or can be generalized across different contexts, cross-category classification evaluates the transferability of the classification model.

2.4.2. *Representational dissimilarity analysis*

The representational similarity analysis (Haxby et al., 2014; Kriegeskorte, 2008; Popal et al., 2019) was based on a 24 × 24 representational dissimilarity matrix structure, with rows and columns representing the combinations of the 8 stimulus types and the 3 memory conditions (RSA, Fig. 2). To establish predictor matrices, each representing different cognitive models, seven matrices were constructed. The first, "stimulus type" matrix was designed to contrast each stimulus category against all others, disregarding memory conditions. The "seen/unseen" model was constructed to discern old items (those seen during the study phase) from study phase items and new items encountered during the test phase (i.e., encountered for the first time). The "memory condition" model presumed dissimilarity across all three memory conditions: study, old, and new. In addition to these models, three more matrices were created to contrast the three memory conditions individually: old/new, study/old, and study/new.

The creation of neural representational dissimilarity matrices followed a cross-participant pairwise classification scheme. Here, for each participant, the training process utilized aggregated data from all other participants. For every stimulus pair (for example, study-faces and new-houses), classifiers were trained on data from *n*-1 participants and subsequently tested on the left-out participant. This iterative train-test procedure was carried out for all time points and stimulus pairs.

Model correlations were then computed using rank correlations on unfolded neural representational dissimilarity matrices at each time point, along with the model (predictor) dissimilarity matrices. This process generated a time-series of Spearman rho-values for each model in every participant. Subsequently, these values were Fisher-transformed and aggregated across participants for statistical analysis.

Hemispheric differences were further explored by averaging model correlations within participants between 100 and 1000 ms, and comparing the values so obtained using two-sided, paired-sample *t*-tests.

2.4.3. *Memory condition classification*

Two sets of analyses were performed, utilizing a cross-participant (leave-one-subject-out) and cross-stimulus-type (leave-one-category-out) approach. The first involved a three-class analysis (Fig. 3**A**) to examine classification performance for study, old, and new items. Training included aggregated data from *n*-1 participants for all stimulus types except one, allowing the classifiers to categorize memory conditions (study, old, new; chance: 1/3), with subsequent testing on the omitted stimulus type in the left-out participant. This iterative process was repeated for all stimulus types, time-points, and participants. Average classifier performance was also computed across stimulus types at each time point for each participant.

The second set of analyses consisted of binary (two-class) classification analyses (Fig. 3**B**) that focused on specific pairs of conditions. These pairwise analyses included old/new, study/old, and study/new conditions (chance: 1/2). Training included aggregated data from *n*-1 participants for all stimulus types except one, followed by testing on the omitted stimulus type in the participant left out. This iterative process was repeated for stimulus types, time-points, and participants, and all three contrasts. Additionally, average classifier performance was computed across stimulus types at each time point for each participant, for all three contrasts.

Time-resolved Classification. We performed time-resolved classification analyses (Grootswagers et al., 2017) utilizing data from all sensors alongside predefined regions of interest (ROIs). To define these ROIs, we followed the methods previously described by Ambrus et al. (Ambrus et al., 2019, 2021; Ely & Ambrus, 2025) and Dalski et al. (2023; 2022; 2022), with six scalp locations along the median (left and right) and coronal (anterior, central, and posterior) planes.

Spatio-temporal Searchlight. To gain a finer-grained understanding of the spatio-temporal dynamics of information processing, time-resolved analyses were supplemented by sensor-space searchlight analyses. In the searchlight analyses, we systematically examined each channel individually by training and testing the classifier using data from the specific sensor and its adjacent electrodes, effectively performing a time-resolved analysis for each channel.

2.4.4. *Within and cross-task classification*

In addition to the main analyses, two additional within- and cross-task classification analyses were carried out, using the same leave-one-subject-out approach described above. Here, data from the two experimental familiarization tasks (faces-bodies-houses-toys and animals-

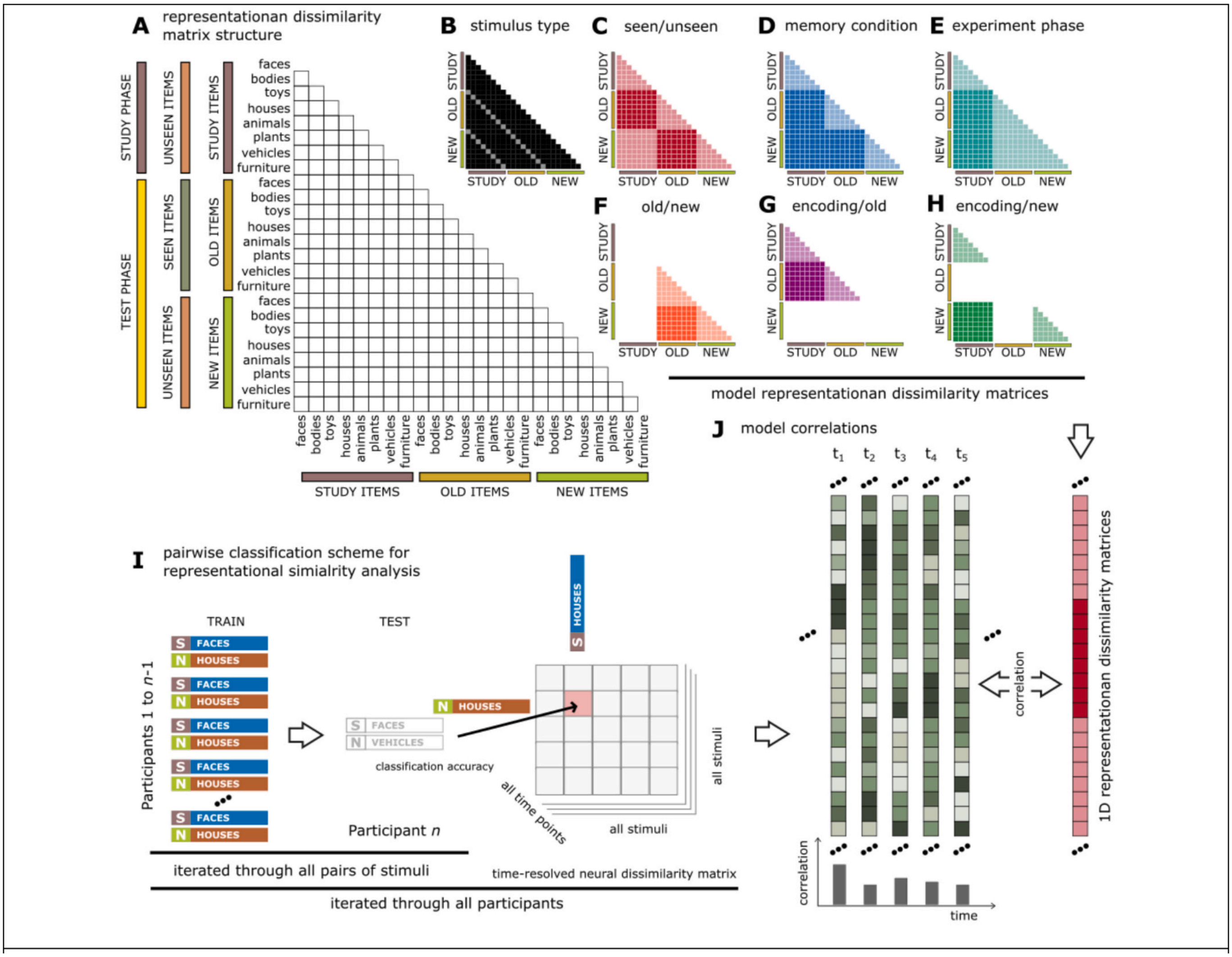

Fig. 2. Cross-participant representational similarity analysis. (**A**) Representational Dissimilarity Matrix structure. The matrix consists of a 24 (8 stimulus types × 3 memory conditions) × 24 grid, with an empty off-diagonal and diagonal. Predictor representational dissimilarity matrices were modelled by filling the grids-points of this with 0 s for similar stimulus-pairs, and with 1 s for dissimilar stimulus-pairs. Seven prediction matrices were created. The stimulus type matrix (**B**) contrasts each stimulus category with the rest of the stimuli, irrespective of memory condition. The seen/unseen model (**C**) contrasts data from old items in the test phase (i.e., seen in the study phase) with data from items in the study phase and new items in the test phase (i.e., items seen for the first time by the participant). The memory condition model (**D**) assumes dissimilarity between all three memory conditions (i.e., study data is different from old and is different from new). The experiment phase model (**E**) contrasts data from the study phase and the test phase of the experiment (i.e., study is different from old and new, old and new are similar). Three additional predictor matrices were constructed to contrast the three memory conditions separately: old/new (**F**), study/old (**G**), study/new (**H**). The creation of the neural representational dissimilarity matrices followed a cross-participant pairwise classification scheme (**I**). For each participant, training was performed on aggregated data from all other participants. For each stimulus pair (e.g., study-faces and new-houses) classifiers were trained on data from *n*-1 participants and tested on the participant left out. This procedure was repeated for all time points and stimulus pairs. Model correlations (**J**) were performed using rank correlations on unfolded neural representational dissimilarity matrices at each time point, and the model (predictor) dissimilarity matrices, resulting in a time-series of Spearman *rho*-values for each model in each participant. These were then Fisher-transformed and aggregated for statistical analysis.

plants-vehicles-furniture) were treated separately. Classifiers were trained to categorize memory conditions (study, old, or new) and pairs of memory conditions (old/new, study/old, study/new) using data from *n*-1 participants and then tested on the participant left out. Within-task analyses involved training and testing data drawn from the same task, while cross-task analyses entailed training on data from one task and testing on the other. This enabled assessment of classifier performance across tasks and participants, further elucidating the generalizability of memory condition classification. The results of these analyses are reported in **Supplementary Information 1**.

2.4.5. *Statistical testing*

To enhance the signal-to-noise ratio, a moving average with a window size of 25 ms (equivalent to 5 consecutive time-points) was applied to all participant-level classification accuracy data. For the ROI-based analyses, the decoding accuracies were subjected to two-tailed, one-sample cluster permutation tests with 10,000 iterations, comparing them against chance levels of 50 % or 33 %. In the searchlight analyses, two-tailed spatio-temporal cluster permutation tests with 10,000 iterations were utilized to compare the results against chance levels.

The statistical analyses were conducted using python, MNE-Python (Gramfort et al., 2013, Gramfort et al., 2014), scikit–learn (Pedregosa et al., 2011) and SciPy (Virtanen et al., 2020).

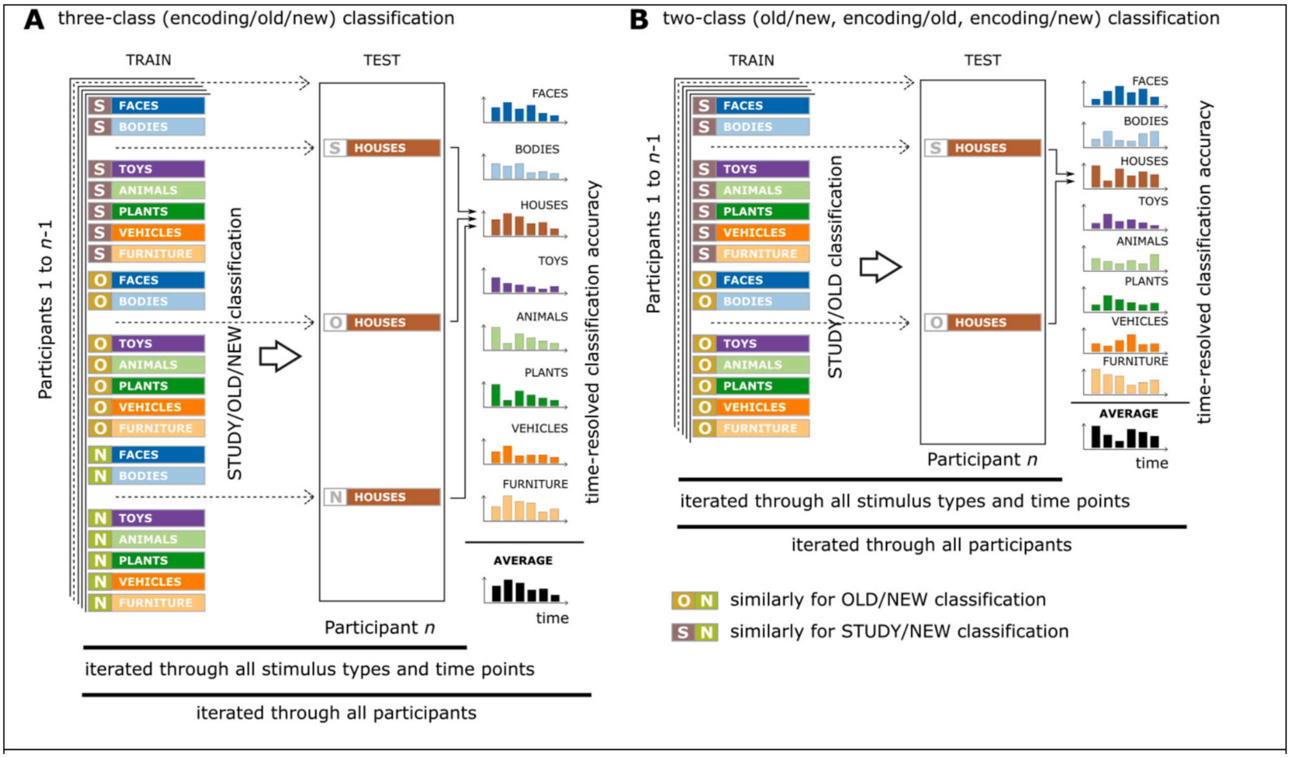

Fig. 3. Cross-participant (leave-one-subject-out), cross-stimulus-type (leave-one-category-out) classification. Classifiers were trained on combined data from all participants, excluding one, and tested iteratively on the excluded participant. In the three-class cross-classification analysis (**A**), training included data for all stimulus types except one, categorizing memory conditions (study/old/new) and testing on the omitted stimulus type. For two-class cross-classification (**B**), training encompassed data for all stimulus types except one, categorizing memory conditions (i.e., old/new, study/old, study/new) and testing on the omitted stimulus type. This process was repeated for all stimulus types and time-points. Time-resolved classifier accuracy scores were recorded for each stimulus type, with an average calculated across types at each time point. These time-series data were aggregated across participants for statistical analysis.

3. Results

3.1. Representational dissimilarity analysis

Stimulus type. The cluster permutation tests conducted on the representational similarity analysis for stimulus type revealed significant results across all regions of interest. Over all electrodes, significant clusters were identified from 80 to 680 ms (cluster $p < 0.0001$), 700 to 980 ms (cluster $p = 0.0058$), and 1055 to 1185 ms (cluster $p = 0.0232$) with peak latencies at 145, 835 and 1125 ms.

Seen/unseen. For the seen/unseen model, significant clusters were identified across all regions of interest. Over all electrodes, a significant cluster was identified from 290 to 700 ms (cluster $p = 0.0003$), peaking at 570 ms.

Memory condition. All regions of interest yielded significant clusters for the memory condition model. For all electrode, a significant cluster was observed from 290 to 1030 ms (cluster $p < 0.0001$), with a peak latency at 550 ms.

Experiment phase. Neither left, nor right anterior regions of interest yielded significant clusters for the experiment phase model. Other regions of interest yielded significant clusters which included time points starting from ca. 300 ms. Over all electrodes, two significant clusters were observed from 270 to 485 ms (cluster $p = 0.0101$) and 525 to 875 ms (cluster $p = 0.0025$), with peak latencies at 365 ms and 735 ms, respectively.

Comparing these models, no significant differences were seen over all electrodes. In the regions of interest, the right anterior area yielded the most consistent differences between ca. 300 and 600 ms.

Old/new. For the old/new model, significant clusters were identified across all regions of interest, generally starting around 200——500 ms. In all electrodes, a significant cluster was identified from 370 to 615 ms (cluster $p = 0.0011$), with a peak latency at 550 ms.

Study/old. All regions of interest yielded significant clusters for the study/old model, with cluster onsets at around 250 – 400 ms. Considering all electrodes, two significant clusters were identified from 255 to 870 ms (cluster $p < 0.0001$) and 895 to 1010 ms (cluster $p = 0.0495$), with peak latencies at 555 ms and 995 ms, respectively.

Study/new. As in the experiment phase model, neither left, nor right anterior regions of interest yielded significant clusters for the study/new model, and no significant clusters were seen in the right central area. Considering all electrodes, two significant clusters were identified from 355 to 425 ms (cluster $p = 0.0462$) and 905 to 1030 ms (cluster $p = 0.0365$), with peak latencies at 375 ms and 945 ms, respectively.

In comparing these models, study/old vs. old/new yielded significant effects in all regions of interest, apart from the anterior ROIs. Over all electrodes, a significant cluster included time points between 225 and 845 ms (peak latency at 450 ms, cluster $p < 0.0001$). For study/old vs. study/new, the time window in which a significant cluster was observed spanned 215 to 670 ms, with a peak latency at 565 ms (cluster $p < 0.0001$). No significant differences were observed for old/new vs. study/new for all electrodes, the right anterior ROI, however, yielded a significant cluster between 360 and 605 ms (peaking at 485 ms, cluster $p = 0.0045$), as well as the left central ROI, between 600 to 705 ms (with a peak at 615 ms, cluster $p = 0.042$).

Onsets, peak latencies and effect sizes, with further, detailed statistics can be found in Supplementary Table 1.

To explore hemispheric differences in the results of the representational similarity analyses, we averaged model correlation values in the regions of interest between 100 and 1000 ms and compared these across the two hemispheres.

Most models yielded positive correlations in general over all regions of interest (Fig. 5**A**). Notable departure from this trend included the

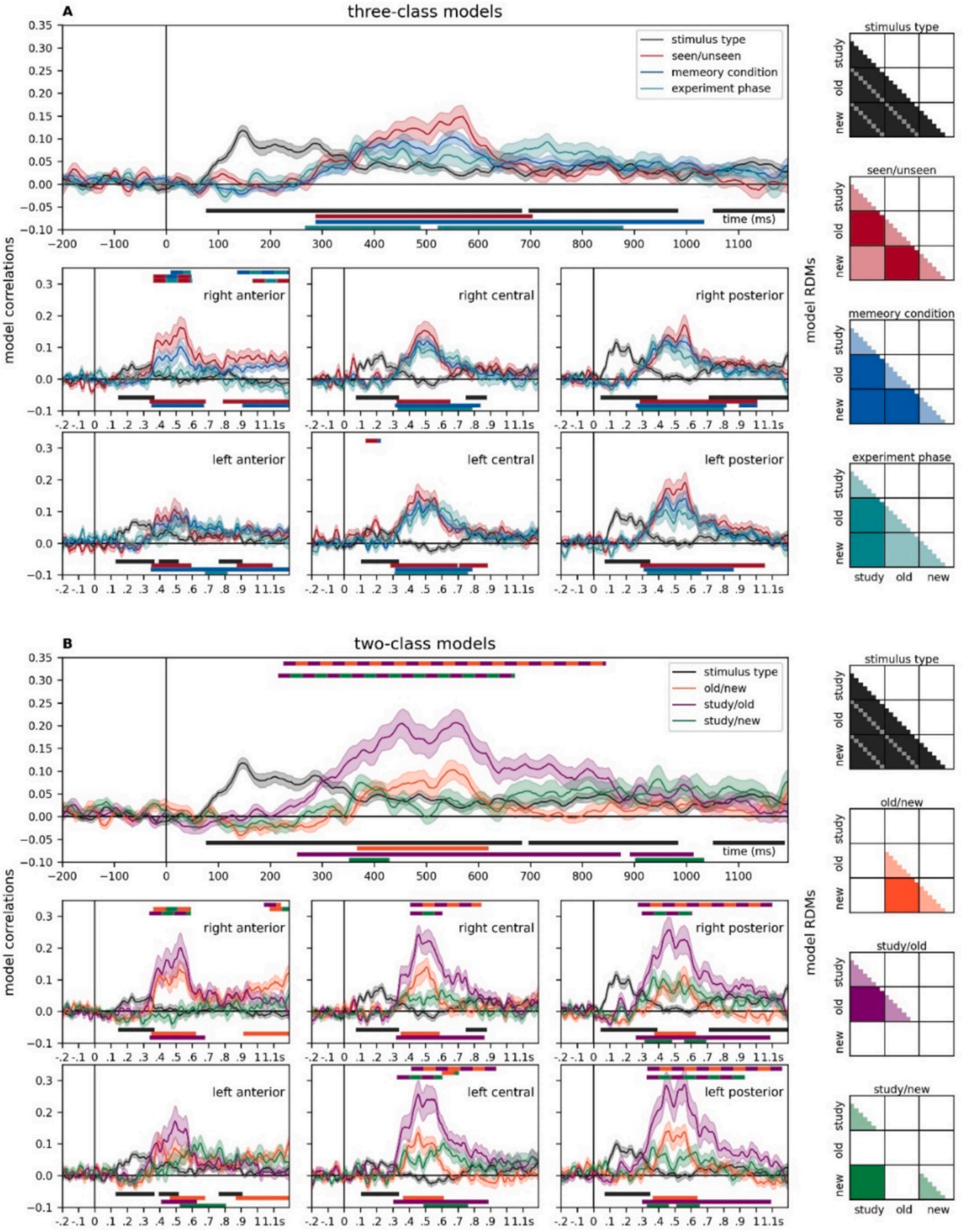

Fig. 4. Leave-one-participant-out representational similarity analysis. (**A**) Results of the three-class models: seen/unseen (old vs. study and new, in red), memory condition (study vs. old vs. new, in blue), and experiment phase (study vs. old and new, in turquoise). (**B**) Results of the two-class models: old/new (in light red), study/old (in purple) and study/new (in green). Results for the stimulus type model shown for comparison (black markers). Shaded ranges denote standard errors of the mean. Significance markers denote the results of two-sided cluster permutation tests, $p < 0.05$. Top panels show results for analyses on all electrodes. Bottom panels: ROI analyses. The same analysis as in the top panel, repeated for the pre-defined regions of interest separately. For detailed statistics, see Supplementary Table 3.

right anterior area where close-to-zero overall model correlations have been observed for the experimental phase and study/new models. Comparing average model correlations between right and left ROIs (Fig. 5**B**), the anterior area demonstrated a right hemispheric dominance for the seen/unseen model ($p = 0.0355$, Cohen's $d = -0.4791$), and left hemispheric bias in the experimental phase ($p = 0.0075$, Cohen's $d = 0.6305$) and study/new ($p = 0.0074$, Cohen's $d = 0.6323$) models. An additional difference in hemispheric bias was observed for the old/new model over the posterior areas, with higher model correlations on the left side ($p = 0.0237$, Cohen's $d = 0.5198$).

3.2. *Classification: study, old, new*

In the 3-class (study/old/new) leave-one-category-out cross-classification analysis, significant clusters were observed in all regions of interest when averaging classification accuracy scores across all stimulus types (Fig. 6, black markers). In the left anterior region, significant clusters were detected from 305 to 780 ms (cluster $p = 0.0015$) and 865

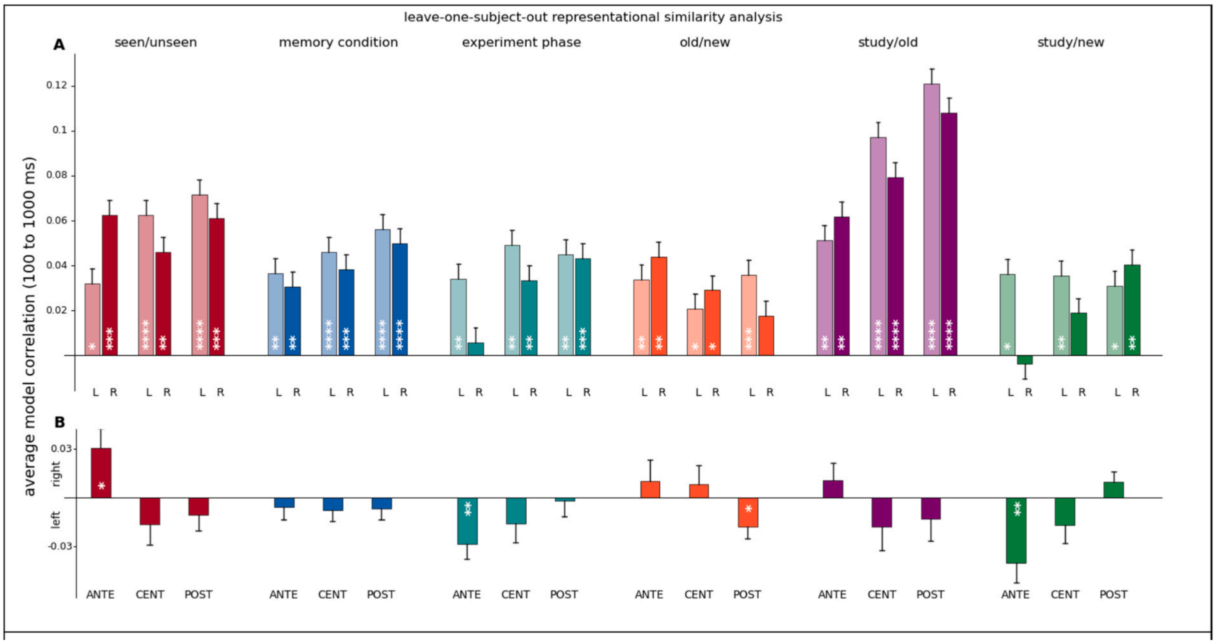

Fig. 5. Leave-one-participant-out representational similarity analysis average model correlations between 100 and 1000 ms. (**A**) Model correlations (see Fig. 5) averaged in the left and right regions of interest, compared to zero using two-sided one-sample *t*–tests. Close-to-zero model correlations were seen for the right anterior ROI for the experiment phase and study/old models. (**B**) Difference between the right and left regions of interest, with comparisons using two-sided paired *t*-tests. A right-hemisphere dominance ($p = 0.036$) in the anterior region was seen for the seen/unseen model, and a more left-anterior hemispheric weight was observed for the experiment phase ($p = 0.0075$) and study/new ($p = 0.0074$) models. Further left-hemisphere bias was present in old/new ($p = 0.024$) in the posterior ROIs. Error bars denote ± standard errors. L/R: left/right. Regions of interests: ANTE: anterior, CENT: central, POST: posterior. Asterisks denote uncorrected *p*–values, $^{*}p < 0.05$, $^{**}p < 0.01$, $^{**}p < 0.001$, $^{***}p < 0.0001$, $^{****}p < 0.00001$.

to 1190 ms (cluster $p = 0.0101$), with peak latencies at 495 ms and 980 ms, respectively. In the right anterior region, a significant cluster was identified from 350 ms to the end of the epoch (cluster $p < 0.0001$), with a peak latency at 495 ms. In the left central region, a significant cluster was observed from 345 to 815 ms (cluster $p < 0.0001$), with a peak latency at 505 ms. In the right central region, two significant clusters were found from 290 to 1025 ms (cluster $p < 0.0001$) and 1080 ms to the end of the epoch (cluster $p = 0.048$), with peak latencies at 495 ms and 1135 ms, respectively. In the left posterior region, significant clusters occurred from 120 to 250 ms (cluster $p = 0.0435$) and 280 to 860 ms (cluster $p < 0.0001$), with peak latencies at 155 ms and 455 ms, respectively. In the right posterior region, a significant cluster was detected from 265 to 1060 ms (cluster $p < 0.0001$), with a peak latency at 560 ms. Over all electrodes, a single significant cluster was identified from 270 ms to the end of the epoch (cluster $p < 0.0001$), with a peak latency at 455 ms. In the searchlight analysis, a single significant spatiotemporal cluster was identified, starting at 80 ms, with a peak at 445 ms over electrode POz (cluster $p < 0.0001$, peak Cohen's $d = 1.52$).

For the various stimulus types, with the exception of the plants category, all analyses yielded significant clusters over all electrodes (Fig. 6, colored markers), with the earliest onset at 340 ms for faces, and cluster *p*-values ranging from < 0.0001 for toys and 0.0325 for furniture, in the earliest significant clusters. In the spatiotemporal searchlight analyses, all stimulus types yielded significant clusters; with cluster *p*-values ranging from < 0.0001 to 0.0263, with the earliest onset seen for toys at 100 ms, and a latest for plants at 335 ms.

In the pre-defined regions of interest, all stimulus types yielded significant clusters in the left and right posterior areas, with an overlap across the stimulus types between ca. 400 and 500 ms. No significant clusters were seen for plants and furniture in the right central, and for toys in the left central region of interest. The right anterior region of interest yielded significant clusters only for bodies, toys and furniture, while in the left anterior region only faces, bodies, toys, and furniture yielded significant clusters.

Onsets, peak values, and further, detailed statistics can be found in Supplementary Table 2. Cross-task classification results exhibited very similar patterns. These results are reported in **Supplementary Information 1**, and detailed statistics can be found in Supplementary Table 4.

3.3. *Classification: old/new, study/old, study/new*

Old/new. In the old/new, leave-one-category-out cross-classification analysis, significant clusters were observed in all regions of interest when averaging classification accuracy scores across all stimulus types (Fig. 7, black markers). These were observed 300 ms following stimulus onset. Over all electrodes, two significant clusters were found from 365 to 640 ms (cluster $p = 0.0024$) and 930 to 1050 ms (cluster $p = 0.0399$), with peak latencies at 545 ms and 945 ms, respectively. The spatiotemporal searchlight analysis identified a significant cluster spanning from 300 ms to the end of the epoch (cluster $p = 0.0002$), with the peak occurring at 545 ms over channel P3 (peak Cohen's $d = 1.357803$).

Study/new. In the study/new contrast, averaged across all stimulus types, significant clusters were observed for all regions of interest (Fig. 7, blue markers). The onset of these clusters was around 300 ms in the central and posterior regions of interest, while onsets around 600–800 ms were seen over anterior regions. Over all electrodes, a significant cluster was observed from 270 ms to the end of the epoch (cluster $p < 0.0001$) with a peak latency at 450 ms. The spatiotemporal searchlight analysis detected a significant cluster spanning the epoch from 265 ms (cluster $p < 0.0001$), with the peak at 450 ms over channel Pz (peak Cohen's $d = 1.153958$).

Study/old. In the study/old contrast, averaged across all stimulus types, significant clusters were observed for all regions of interest (Fig. 7, red markers). The onset of these clusters was around 250–300 ms, apart from the left posterior ROI, where the significant cluster included time points starting from 140 ms. Considering all electrodes, a significant cluster was detected from 155 to 1185 ms (cluster $p < 0.0001$) with a peak latency at 460 ms. The spatiotemporal searchlight

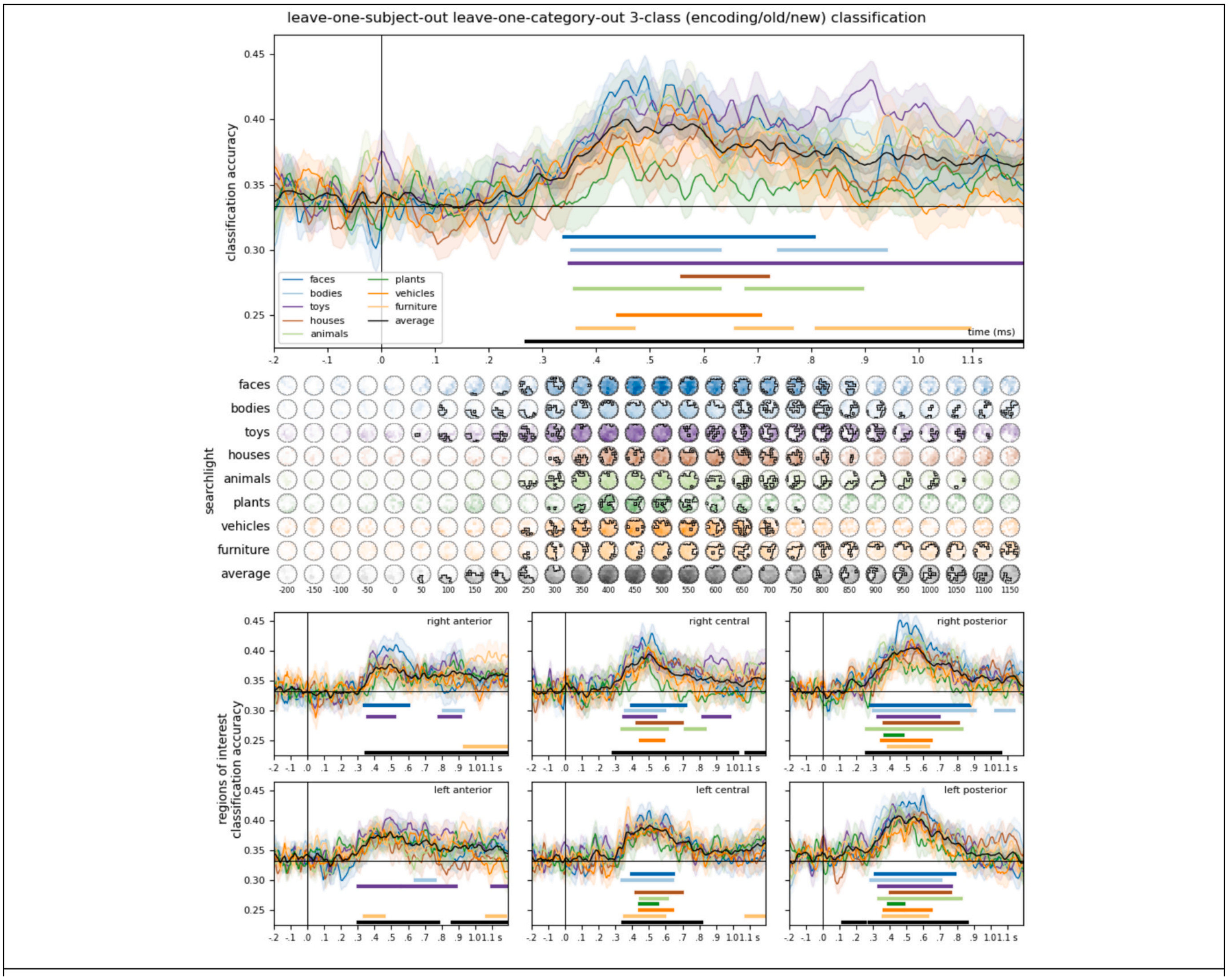

Fig. 6. Cross-participant, study/old/new leave-one-category-out cross-classification analysis for the different stimulus types (colored lines), and accuracy scores averaged across stimulus types (black line). Classifiers were trained to categorize memory condition (study, old or new) on data from n-1 participants and tested on the participant left out. For the train-test split, one stimulus category was iteratively held out for testing. Shaded ranges denote standard errors of the mean. Significance markers denote the results of two-sided cluster permutation tests, $p < 0.05$. Top panel shows results for analyses on all electrodes. Middle panels: spatio-temporal searchlight results are shown as scalp maps, with classification accuracy scores averaged in 50 ms steps. Sensors and time points forming significant clusters are marked (two-sided spatio-temporal cluster permutation tests, $p < 0.05$). Bottom panels: ROI analyses. The same analysis as in the top panel, repeated for the predefined areas separately. For detailed statistics, see Supplementary Table 2.

analysis yielded a significant cluster spanning the epoch from 95 ms (cluster $p < 0.0001$), with the peak observed at 450 ms on channel PO3 (peak Cohen's $d = 1.58832$).

Comparisons between contrasts. In the comparison, over all electrodes, between study/old and old/new conditions, a significant cluster was found in the time window from 270 to 810 ms, with a peak latency at 655 ms (cluster $p < 0.0001$). In the comparison between study/old and study/new conditions, a significant cluster was observed in the time window from 370 to 595 ms, with a peak latency at 560 ms (cluster $p = 0.0077$). No significant clusters were identified in the comparison between old/new and study/new conditions over all electrodes, however, a significant cluster was seen in the right anterior region of interest between 315 and 525 ms (cluster $p = 0.0107$). The left anterior region of interest did not yield any significant effects in the comparisons between contrasts.

Onsets, peak values and effect sizes, and further, detailed statistics can be found in Supplementary Table 3.

The within and cross-task classification results mirrored the average outcomes observed across individual stimulus types described above. Notable departures from this, across all electrodes, included a significant difference between old/new and study/new in the faces-bodies-houses-toys task within the approximate 300–400 ms window, along with no significant difference between old/new and study/old in the ca. 350 to 600 ms range. Within the animals-plants-vehicles-furniture task, the encoding/new effect was observed considerably later (ca. 1000 ms), and only a late significant differentiation between old/new and study/old was seen. Results are reported in more detail in **Supplementary Information 1**, with statistics in Supplementary Table 5.

3.4. *The representations of stimulus type in the different memory conditions*

The representations of stimulus type across different memory conditions were examined using pairwise classification accuracies derived from the neural representational dissimilarity matrix calculated for the representational similarity analysis. When considering all stimulus types

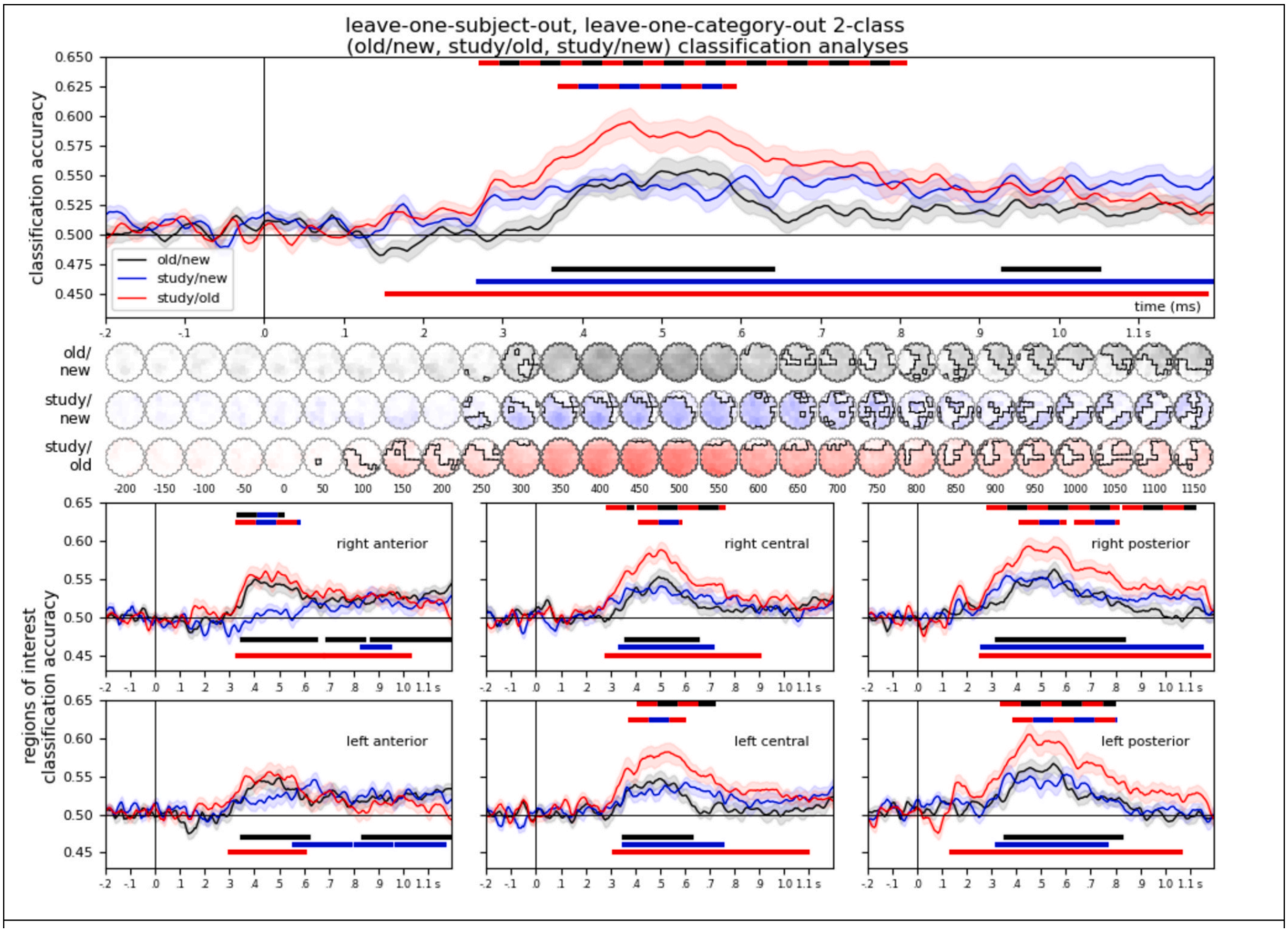

Fig. 7. Cross-participant, old/new, study/old, study/new leave-one-category-out cross-classification analyses for accuracy scores averaged across the eight stimulus types. Classifiers were trained to categorize pairs of memory conditions (old/new: black markers, study/old: red markers, study/new: blue markers) on data from *n*-1 participants and tested on the participant left out. For the train-test split, a stimulus category was iteratively held out for testing. Shaded ranges denote standard errors of the mean. Significance markers denote the results of two-sided cluster permutation tests, $p < 0.05$. The top panel shows results for analyses on all electrodes. Middle panels: spatio-temporal searchlight results are shown as scalp maps, with classification accuracy scores averaged in 50 ms steps. Sensors and time points forming significant clusters are marked (two-sided spatio-temporal cluster permutation tests, $p < 0.05$). Bottom panels: ROI analyses. The same analysis as in the top panel, repeated for the pre-defined areas separately. For detailed statistics, see Supplementary Table 3.

together, consistent effects were observed across all memory conditions, although no statistically significant difference emerged between these conditions across all electrodes. However, when analyzing faces-houses-bodies-toys separately, stimulus type classification was most pronounced in the old condition, showing a significant difference from the new condition starting around 400 ms. Conversely, in animals-plants-vehicles-furniture, a late (680 to 795 ms) difference was observed between the new and old conditions, with stimulus type being better decodable in the new memory condition. Interestingly, when testing all stimulus types separately, only faces exhibited consistent differences between old and new conditions, resulting in significant clusters between 775 and 960 ms and 980 to 1105 ms. See **Supplementary Information 2** for further details.

To better illustrate the trends in the time-course of stimulus type representations, we averaged pairwise classifier performance in each memory condition for each participant in the 100 ms to 1000 ms post-stimulus-onset time range for all stimulus types (Fig. 8**A**), for the two tasks (faces, bodies, houses, toys and animals, plants, vehicles, furniture) separately (Fig. 8**B**), and all stimulus types separately (Fig. 8**C**). For statistics, see in **Supplementary Information Table S5.**

4. Discussion

The objective of this study was to investigate the shared neural dynamics underlying memory encoding and recognition processes across different visual stimulus types for short-term experimental familiarization. For this aim, we employed pairwise leave-one-subject-out classification for the representational similarity analyses, and a combination of leave-one-subject-out and leave-one-category-out procedures for multivariate cross-classification. The main findings of our study are as follows: 1) In representational similarity analyses, stimulus type effects manifested first, around 80 ms post-stimulus onset and reached their peak magnitude at approximately 140 ms. This observation is consistent with previous research, indicating rapid neural differentiation based on stimulus characteristics. 2) Stimulus type effects gradually transitioned to memory-related effects around 300 ms post-stimulus onset. 3) Alongside old/new effects, we observed effects related to the experiment phase (study vs. test) and the differentiation between seen and unseen stimuli. 4) In cross-classification, study/old effects were evident as early as 155 ms post-stimulus onset, suggesting an early differentiation between items at study and previously studied stimuli. In contrast, old/new effects predominantly emerged in the 400 to 600 ms time range, with study/new effects falling between these two effects.

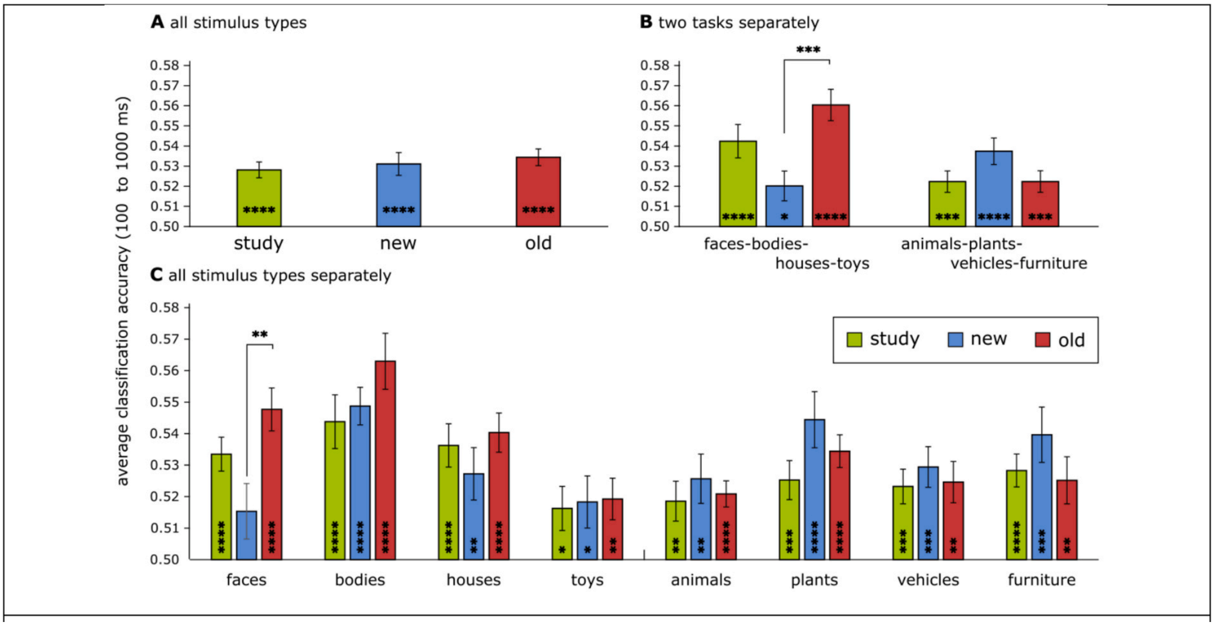

Fig. 8. Stimulus type classification in the three memory conditions. Pairwise classification accuracies are averaged between 100 and 1000 ms over all electrodes (**A**) for all stimulus types, (**B**) for the two tasks (faces, bodies, houses, toys and animals, plants, vehicles, furniture) separately, and (**C**) all stimulus types separately. Generally, stimulus type was well-classified in all memory conditions (one-sample two-tailed *t*-test against chance). No statistically significant difference was observed for all stimulus types. In faces-bodies-houses-toys, stimulus type classification accuracy was significantly higher for old compared to new stimuli ($t = 3.98$, $p = 0.0007$). In animals-plants-vehicles-furniture, new stimuli were better classified, although the contrast was not statistically significant ($t = 1.84$, $p = 0.08$). For all stimulus types separately, only face stimuli yielded a significant difference in memory effects, where classification accuracy for old stimuli were significantly higher than new stimuli ($t = 2.98$, $p = 0.008$). Paired *t*-tests. $^{*}p_{\text{uncorrected}} < 0.05$, $^{**}p_{\text{uncorrected}} < 0.01$, $^{***}p_{\text{uncorrected}} < 0.001$, $^{****}p_{\text{uncorrected}} < 0.0001$. Error bars denote ± SEM. For data, see Supplementary Information Table S5A, B and C.

4.1. *The time-course of shared stimulus and memory-related effects*

Shared effects of stimulus type. The cross-participant representational similarity analysis revealed model correlations with the stimulus type model, with a significant cluster onset observed at approximately 80 ms, reaching its peak around 140 ms. Early visual stimulus category effects are consistently reported in the literature. For instance, Wang et al. (2012) noted above-chance category discrimination beginning around the P1 range and peaking in the N1/N170 window in an EEG experiment featuring human faces, buildings, cats, and cars. Carlson et al. (2013) detected decoding onsets and peaks at approximately 80 and 100 ms using MEG decoding in a study presenting animal bodies, animal faces, human bodies, human faces, man-made objects, and natural objects. In an MEG decoding investigation, van de Nieuwenhuijzen et al. (2013) reported category classification peaked in the first 100 to 200 ms after stimulus onset for faces, scenes, bodies, and tools. Similarly, Cichy et al. (2014) utilized MEG RSA with human and nonhuman faces and bodies, as well as natural and artificial objects, finding peaks in category membership between approximately 120 and 170 ms. Using EEG RSA, Kaneshiro et al. (2015) examined faces, bodies, fruits, vegetables, animal faces and bodies, and objects, identifying peak accuracy in category-level classifications from 144 to 224 ms. Employing RSA on EEG data for faces, houses, toys and bodies, Xie et al. (2022) found a significant cluster onset at 72 ms and a peak at 154 ms. In a recent study, Klink et al. (2023) reported face-scene discrimination beginning around 100 ms and peaking at 160 ms in an EEG decoding study. Our findings are consistent with these results, adding to the body of evidence regarding early neural processing of stimulus categories. Moreover, our present observations further highlight that these effects are shared across participants.

Shared memory-related effects. In our previous study (Ambrus, 2024) we employed multivariate cross-dataset classification analysis to explore shared signals of recognition memory, probing the patterns of neural activity shared across different memory tasks, stimulus types and datasets. We found that shared signature of memory recall overlapped between ca. 400–600 ms irrespective of stimulus type and the age of the memory trace. Here, we aimed at a more systematic investigation of shared neural signatures of memory processes, including the encoding phase, for short-term familiarity.

In this present study, memory-related effects in the representational similarity analyses first manifested around 250 – 300 ms, plateaued and peaked in the ca. 400 to 600 ms range (Fig. 4). In previous studies, the initial rapid feedforward signal, indicated by a sharp peak in classification performance, has been shown to be mainly driven by low-level stimulus properties (Ambrus et al., 2019; Dalski et al., 2022b). Subsequently, there is a decline in classifier performance, transitioning to a more gradual and sustained effect at around 200 to 600 ms (Klink et al., 2023). This later phase is hypothesized to be influenced by the integration of more detailed feedback from higher cortical areas (Contini et al., 2017). It should be noted, however, that evidence exists for a modulation of the early phase of this signal (<200 ms) by familiarity with the stimulus, particularly for pre-experimentally familiar (famous) faces (Dobs et al., 2019). In the study by Speer and Curran (2007), the P1 ERP component, occurring around 100–175 ms after stimulus onset and observed at bilateral inferior/parietal regions (LPI and RPI) on the scalp was found to be indicative of item familiarity during initial perceptual processing, distinguishing between new and known items at an early stage of visual processing.

The memory-related effects observed in our current investigation are in line with those reported in the literature. In both our representational similarity analyses and cross-classification analyses we found stable old/new effects between 400–600 ms that are consistent with previous studies (Ambrus, 2024; Dobs et al., 2019) and align with the parietal old/new effect often associated with recollection (Kwon et al., 2023; Rugg & Curran, 2007; Rugg & Yonelinas, 2003).

However, in contrast to our within-category RSA findings, in our cross-stimulus-category classification analyses, study/old effects emerged much earlier, around 150 ms in the time-resolved analysis and approximately 100 ms in the searchlight analysis. These effects were most prominent in the posterior areas of the left hemisphere. This earlier manifestation of memory effects is likely attributable to the larger training set in cross-classification compared to the RSA and is thus further indicative of shared memory-related processing across stimulus types.

Hemispheric asymmetries

In our current study, the most significant hemispheric asymmetries were observed in the anterior regions of interest (see Fig. 6 and **Supplementary Fig. S5**). Differential processing in frontal brain areas has been consistently documented in relation to memory functions. Early models, such as the hemispheric encoding and retrieval asymmetry (Tulving et al., 1994), posited a relative difference in engagement of the left and right prefrontal cortices during episodic memory processes. Specifically, according to this model, the left prefrontal cortex (PFC) is predominantly implicated in the encoding phase, whereas the right PFC is primarily involved in retrieval (Habib et al., 2003). While this pattern has been observed across various types of stimuli, the evidence is far from equivocal (see e.g., Andreau & Torres Batán, 2019; Kelley et al., 1998; Wagner et al., 1998). Using representational similarity analysis in the present study allowed for a more in-depth exploration not only of the encoding and recall stages but also of the distinct contributions of both novel and old items.

The effects of experimental phase and memory conditions over both the left and right frontal regions of interest revealed a complex pattern. The left hemisphere showed a greater ability to differentiate between items being studied and novel items during the test phase, while the right hemisphere was more sensitive to distinguishing between seen and unseen items, with no clear advantage in the old vs. new contrast. Additionally, the contrast between study and test phases was left-lateralized.

In the time-resolved RSA analysis, overall, all regions of interest exhibited effects distinguishing between seen and unseen items, memory conditions, as well as between old and new items. Moreover, prominent effects have been observed for items under study and those encountered during the test phase. However, both the left and right frontal regions of interest demonstrated a low sensitivity to the experimental phase and the differentiation between items under study and new items during the test phase (Fig. 4). Further examining hemispheric differences in the averaged time-course of the model correlations (Fig. 5) indications of differential processing in the anterior ROIs were observed. Here, the analysis revealed higher average model correlations in the right hemisphere for seen (old) versus unseen (i.e., study and novel) items, and higher model correlations in the left hemisphere for both the experimental phase (study versus old and novel) and for the study versus new models. Comparable patterns emerged in cross-classification: the right anterior region of interest exhibited little discernible study/new effects, while both old/new and study/old effects were notably more pronounced than study/new effects in the ca. 300 to 600 ms window (Fig. 7).

The observed effects suggest a more nuanced picture than the straightforward left/right encoding/recognition dichotomy would predict. One possible explanation is that encoding processes can still occur during recall tasks, even when study instructions are not explicitly given (Vogelsang et al., 2016). To further investigate this, future studies could implement a surprise recall task for novel items in the test phase to determine the nature of the encoding processes that are active. Additionally, all test-phase items might inherently engage recall processes regardless of the specific task.

4.2. Stimulus type representations in the different memory conditions

In Klink et al. (2023) we observed stronger stimulus category representations for familiar faces and scenes compared to unfamiliar ones. In that report, we highlighted the need for further investigation to ascertain whether this effect extends to other types of stimuli beyond these categories, especially when human faces are absent from the stimulus categories. We set out to test this in our current experiment.

In our results, this appears to be specific to the faces-houses-bodies-toys task, and strongest for face stimuli. Interestingly, in the animals-plants-vehicles-furniture task, the trend is reversed, indicating a marked divergence from this expected pattern. Our present findings indicate that the notion that enhanced stimulus type classification familiar items is not straightforward. While this pattern appears to hold true for face stimuli, it might not necessarily extend to other stimulus types, at least not for short-term, experimental familiarization. Factors such as practice effects or tiredness, stemming from the consistent task order across participants, may also contribute to these results. Furthermore, salience (Cooper et al., 2019), distinctiveness (Waddill & McDaniel, 1998), differential encoding/recall strategies, differences in nameability (Hitch et al., 1995; Madrid et al., 2019), which were not directly examined in our study, could potentially contribute to these differential findings. Further experiments are warranted to elucidate the precise contributions of these factors to the observed patterns.

4.3. Limitations and future directions

Given the high accuracy of responses and confidence levels observed in our study, the exploration of subsequent memory effects and subjective memory strength during encoding and recognition was rendered impractical. Cross-dataset classification evidence (Ambrus, 2024) suggests that the shared neural signals of memory are modulated at recognition time; these should be investigated in relation to subsequent memory effects (Mecklinger & Kamp, 2023). To address this, future studies could adopt designs featuring a larger pool of study items and/or extended intervals between study and test phases. This adjustment would allow for more substantial forgetting to occur, thereby increasing the number of trials available, enhancing statistical power for cross-classification analyses. Here, we conducted a within-experiment, cross-participant analysis, however, similar methodologies can be extended across experiments using different stimuli and paradigms (Ambrus, 2024; Dalski et al., 2023; Dalski et al., 2022b; Dalski et al., 2022a; Li et al., 2022), as well as datasets acquired using the same stimuli and paradigm but with different participant populations, such as adults and children (Xie et al., 2022). This approach not only opens up the possibility to further investigate memory processes, for example extending it to domains other than visual perception, but it also offers opportunities to explore the developmental trajectories of these processes across the lifespan and investigate their alterations in conditions affecting memory.

4.4. Summary

In this study, we explored the shared neural dynamics of encoding and recognition processes across participants and visual object stimulus types for short term familiarization. Our findings replicated previous research, extending it to the encoding of stimuli, revealing early visual stimulus category effects around 150 ms and old/new effects around 400 to 600 ms following stimulus onset. Additionally, we observed a divergence in neural responses for encoding, old, and new stimuli around 300 ms. Specifically, items encountered during the study phase were most distinguishable from old items during the test phase, with discernible effects emerging as early as 150 ms in cross-category classification. Anterior regions of interest, particularly in the right hemisphere, exhibited little differentiation between experimental phases or between study and new items. This suggests that similar processing occurs for items not encountered previously in the experiment. Visual stimulus category representations, investigated here for short-term experimental familiarity, do not consistently adhere to the old >new pattern observed previously in long-term personal familiarity with faces and scenes. Interestingly, this pattern was only statistically significant for experimentally familiarized faces in our study, suggesting a potentially unique phenomenon specific to facial stimuli. Further investigation is needed to elucidate the underlying mechanisms and determine if the effect is face-specific or influenced by other factors. Finally, this study underscores the potential of multivariate cross-classification and cross-dataset classification as promising tools for investigating abstraction and shared neural signatures of cognitive processing.

CRediT authorship contribution statement

Berfin Ozdemir: Writing – review & editing, Writing – original draft, Investigation, Conceptualization. **Géza Gergely Ambrus:** Writing – review & editing, Writing – original draft, Visualization, Supervision, Software, Methodology, Formal analysis, Data curation, Conceptualization.

Declaration of competing interest

The authors declare that they have no known competing financial interests or personal relationships that could have appeared to influence the work reported in this paper.

Appendix A. Supplementary data

Supplementary data to this article can be found online at https://doi.org/10.1016/j.brainres.2025.149616.

Data availability

The data that support the findings of this study are openly available in the The Open Science Framework at https://osf.io/bhuxj/

References

Ambrus, G.G., 2024. Shared neural codes of recognition memory. Sci. Rep. 14 (1), 15846. https://doi.org/10.1038/s41598-024-66158-y.

Ambrus, G.G., Eick, C.M., Kaiser, D., Kovács, G., 2021. Getting to know you: Emerging neural representations during face familiarization. J. Neurosci. 41 (26), 5687–5698. https://doi.org/10.1523/JNEUROSCI.2466-20.2021.

Ambrus, G.G., Kaiser, D., Cichy, R.M., Kovács, G., 2019. The neural dynamics of familiar face recognition. Cereb. Cortex 29 (11), 4775–4784. https://doi.org/10.1093/cercor/bhz010.

Andreau, J.M., Torres Batán, S., 2019. Exploring lateralization during memory through hemispheric pre-activation: Differences based on the stimulus type. Laterality: Asymmetries of Body, Brain and Cognition 24 (4), 393–416. https://doi.org/10.1080/1357650X.2018.1531422.

Bentin, S., Allison, T., Puce, A., Perez, E., McCarthy, G., 1996. Electrophysiological studies of face perception in humans. J. Cogn. Neurosci. 8 (6), 551–565. https://doi.org/10.1162/jocn.1996.8.6.551.

Bötzel, K., Grüsser, O.-J., 1989. Electric brain potentials evoked by pictures of faces and non-faces: a search for ?face-specific? EEG-Potentials. Experimental Brain Research 77 (2), 349–360. https://doi.org/10.1007/BF00274992.

Carlson, T.A., Tovar, D.A., Alink, A., Kriegeskorte, N., 2013. Representational dynamics of object vision: The first 1000 ms. J. Vis. 13 (10), 1. https://doi.org/10.1167/13.10.1.

Cichy, R.M., Pantazis, D., Oliva, A., 2014. Resolving human object recognition in space and time. Nat. Neurosci. 17 (3), 455–462. https://doi.org/10.1038/nn.3635.

Contini, E.W., Wardle, S.G., Carlson, T.A., 2017. Decoding the time-course of object recognition in the human brain: From visual features to categorical decisions. Neuropsychologia 105, 165–176. https://doi.org/10.1016/j.neuropsychologia.2017.02.013.

Cooper, R.A., Kensinger, E.A., Ritchey, M., 2019. Memories fade: the relationship between memory vividness and remembered visual salience. Psychol. Sci. 30 (5), 657–668. https://doi.org/10.1177/0956797619836093.

Curran, T., 1999. The electrophysiology of incidental and intentional retrieval: ERP old/new effects in lexical decision and recognition memory. Neuropsychologia 37 (7), 771–785. https://doi.org/10.1016/S0028-3932(98)00133-X.

Dalski, A., Kovács, G., Ambrus, G.G., 2022a. Evidence for a general neural signature of face familiarity. Cereb. Cortex 32 (12), 2590–2601. https://doi.org/10.1093/cercor/bhab366.

Dalski, A., Kovács, G., Ambrus, G.G., 2023. No semantic information is necessary to evoke general neural signatures of face familiarity: evidence from cross-experiment classification. Brain Struct. Funct. 228 (2), 449–462. https://doi.org/10.1007/s00429-022-02583-x.

Dalski, A., Kovács, G., Wiese, H., Ambrus, G.G., 2022b. Characterizing the shared signals of face familiarity: Long-term acquaintance, voluntary control, and concealed knowledge. Brain Res. 1796, 148094. https://doi.org/10.1016/j.brainres.2022.148094.

Danker, J.F., Hwang, G.M., Gauthier, L., Geller, A., Kahana, M.J., Sekuler, R., 2008. Characterizing the ERP old-new effect in a short-term memory task. Psychophysiology 45 (5), 784–793. https://doi.org/10.1111/j.1469-8986.2008.00672.x.

Delorme, A., 2023. EEG is better left alone. Sci. Rep. 13, 2372. https://doi.org/10.1038/s41598-023-27528-0.

Dobs, K., Isik, L., Pantazis, D., Kanwisher, N., 2019. How face perception unfolds over time. Nat. Commun. 10 (1). https://doi.org/10.1038/s41467-019-09239-1.

Ely, M.M., Ambrus, G.G., 2025. Shared neural dynamics of facial expression processing. Cognitive Neurodynamics 19 (1), 45. https://doi.org/10.1007/s11571-025-10230-4.

Gramfort, A., Luessi, M., Larson, E., Engemann, D.A., Strohmeier, D., Brodbeck, C., Goj, R., Jas, M., Brooks, T., Parkkonen, L., Hämäläinen, M., 2013. MEG and EEG data analysis with MNE-Python. Frontiers in Neuroscience. https://doi.org/10.3389/fnins.2013.00267.

Gramfort, A., Luessi, M., Larson, E., Engemann, D.A., Strohmeier, D., Brodbeck, C., Parkkonen, L., Hämäläinen, M.S., 2014. MNE software for processing MEG and EEG data. Neuroimage 86, 446–460. https://doi.org/10.1016/j.neuroimage.2013.10.027.

Grootswagers, T., Wardle, S.G., Carlson, T.A., 2017. Decoding dynamic brain patterns from evoked responses: A tutorial on multivariate pattern analysis applied to time series neuroimaging data. J. Cogn. Neurosci. 29 (4), 677–697. https://doi.org/10.1162/jocn_a_01068.

Habib, R., Nyberg, L., Tulving, E., 2003. Hemispheric asymmetries of memory: the HERA model revisited. Trends Cogn. Sci. 7 (6), 241–245. https://doi.org/10.1016/S1364-6613(03)00110-4.

Haxby, J.V., Connolly, A.C., Guntupalli, J.S., 2014. Decoding neural representational spaces using multivariate pattern analysis. Annu. Rev. Neurosci. 37 (1), 435–456. https://doi.org/10.1146/annurev-neuro-062012-170325.

Hitch, G.J., Brandimonte, M.A., Walker, P., 1995. Two types of representation in visual memory: Evidence from the effects of stimulus contrast on image combination. Mem. Cogn. 23 (2), 147–154. https://doi.org/10.3758/BF03197217.

Hong, Y., Moore, I.L., Smith, D.E., Long, N.M., 2023. Spatiotemporal dynamics of memory encoding and memory retrieval states. J. Cogn. Neurosci. 35 (9), 1463–1477. https://doi.org/10.1162/jocn_a_02022.

Horner, A.J., Bisby, J.A., Bush, D., Lin, W.-J., Burgess, N., 2015. Evidence for holistic episodic recollection via hippocampal pattern completion. Nat. Commun. 6 (1), 7462. https://doi.org/10.1038/ncomms8462.

Kamp, S.-M., Zimmer, H.D., 2015. Contributions of attention and elaboration to associative encoding in young and older adults. Neuropsychologia 75, 252–264. https://doi.org/10.1016/j.neuropsychologia.2015.06.026.

Kaneshiro, B., Perreau Guimaraes, M., Kim, H.-S., Norcia, A.M., Suppes, P., 2015. A representational similarity analysis of the dynamics of object processing using single-trial EEG classification. PLoS One 10 (8), e0135697. https://doi.org/10.1371/journal.pone.0135697.

Kaplan, J.T., Man, K., Greening, S.G., 2015. Multivariate cross-classification: Applying machine learning techniques to characterize abstraction in neural representations. Front. Hum. Neurosci. 9 (MAR). https://doi.org/10.3389/fnhum.2015.00151.

Kelley, W.M., Miezin, F.M., McDermott, K.B., Buckner, R.L., Raichle, M.E., Cohen, N.J., Ollinger, J.M., Akbudak, E., Conturo, T.E., Snyder, A.Z., Petersen, S.E., 1998. Hemispheric specialization in human dorsal frontal cortex and medial temporal lobe for verbal and nonverbal memory encoding. Neuron 20 (5), 927–936. https://doi.org/10.1016/S0896-6273(00)80474-2.

Klink, H., Kaiser, D., Stecher, R., Ambrus, G.G., Kovács, G., 2023. Your place or mine? The neural dynamics of personally familiar scene recognition suggests category independent familiarity encoding. Cereb. Cortex 33 (24), 11634–11645.

Kriegeskorte, N., 2008. Representational similarity analysis – connecting the branches of systems neuroscience. Front. Syst. Neurosci. 2, 4. https://doi.org/10.3389/neuro.06.004.2008.

Kwon, S., Rugg, M.D., Wiegand, R., Curran, T., Morcom, A.M., 2023. A meta-analysis of event-related potential correlates of recognition memory. Psycho. Bull. Rev. 30 (6), 2083–2105. https://doi.org/10.3758/s13423-023-02309-y.

Li, C., Burton, A.M., Ambrus, G.G., Kovács, G., 2022. A neural measure of the degree of face familiarity. Cortex 155, 1–12. https://doi.org/10.1016/j.cortex.2022.06.012.

Long, N.M., Kuhl, B.A., 2019. Decoding the tradeoff between encoding and retrieval to predict memory for overlapping events. Neuroimage 201, 116001. https://doi.org/10.1016/j.neuroimage.2019.07.014.

Madrid, J., Cunningham, C.A., Robbins, A., Hout, M.C., 2019. You're looking for what? Comparing search for familiar, nameable objects to search for unfamiliar, novel objects. Vis. Cogn. 27 (1), 8–20. https://doi.org/10.1080/13506285.2019.1577318.

Mecklinger, A., Kamp, S.-M., 2023. Observing memory encoding while it unfolds: Functional interpretation and current debates regarding ERP subsequent memory effects. Neurosci. Biobehav. Rev. 153, 105347. https://doi.org/10.1016/j.neubiorev.2023.105347.

Meßmer, J.A., Bader, R., Mecklinger, A., 2021. The more you know: Schema-congruency supports associative encoding of novel compound words. Evidence from event-related potentials. Brain Cogn. 155, 105813. https://doi.org/10.1016/j.bandc.2021.105813.

Mohan, U.R., Zhang, H., Ermentrout, B., Jacobs, J., 2024. The direction of theta and alpha travelling waves modulates human memory processing. Nat. Human Behav. https://doi.org/10.1038/s41562-024-01838-3.

O'Reilly, R.C., Norman, K.A., 2002. Hippocampal and neocortical contributions to memory: advances in the complementary learning systems framework. Trends Cogn. Sci. 6 (12), 505–510. https://doi.org/10.1016/S1364-6613(02)02005-3.

Otten, L.J., Rugg, M.D., 2001. Electrophysiological correlates of memory encoding are task-dependent. Cogn. Brain Res. 12 (1), 11–18. https://doi.org/10.1016/S0926-6410(01)00015-5.

Pedregosa, F., Varoquaux, G., Gramfort, A., Michel, V., Thirion, B., Grisel, O., Blondel, M., Prettenhofer, P., Weiss, R., Dubourg, V., et al., 2011. Scikit-learn: machine learning in Python. J. Mach. Learn. Res. 12 (Oct), 2825–2830.

Popal, H., Wang, Y., Olson, I.R., 2019. A guide to representational similarity analysis for social neuroscience. Soc. Cogn. Affect. Neurosci. 14 (11), 1243–1253. https://doi.org/10.1093/scan/nsz099.

Richter, F.R., Chanales, A.J.H., Kuhl, B.A., 2016. Predicting the integration of overlapping memories by decoding mnemonic processing states during learning. Neuroimage 124, 323–335. https://doi.org/10.1016/j.neuroimage.2015.08.051.

Rossi, S., Innocenti, I., Polizzotto, N.R., Feurra, M., De Capua, A., Ulivelli, M., Bartalini, S., Cappa, S.F., 2011. Temporal dynamics of memory trace formation in the human prefrontal cortex. Cereb. Cortex 21 (2), 368–373. https://doi.org/10.1093/cercor/bhq103.

Rugg, M.D., Curran, T., 2007. Event-related potentials and recognition memory. Trends Cognit. Sci. 11 (6), 251–257. https://doi.org/10.1016/j.tics.2007.04.004.

Rugg, M.D., Yonelinas, A.P., 2003. Human recognition memory: a cognitive neuroscience perspective. Trends Cogn. Sci. 7 (7), 313–319. https://doi.org/10.1016/S1364-6613(03)00131-1.

Smith, D.E., Moore, I.L., Long, N.M., 2022. Temporal context modulates encoding and retrieval of overlapping events. J. Neurosci. 42 (14), 3000–3010. https://doi.org/10.1523/JNEUROSCI.1091-21.2022.

Speer, N.K., Curran, T., 2007. ERP correlates of familiarity and recollection processes in visual associative recognition. Brain Res. 1174, 97–109. https://doi.org/10.1016/j.brainres.2007.08.024.

Staresina, B.P., Wimber, M., 2019. A neural chronometry of memory recall. Trends Cogn. Sci. 23 (12), 1071–1085. https://doi.org/10.1016/j.tics.2019.09.011.

Tanaka, E., Inui, K., Kida, T., Kakigi, R., 2009. Common cortical responses evoked by appearance, disappearance and change of the human face. BMC Neurosci. 10 (1), 38. https://doi.org/10.1186/1471-2202-10-38.

Teyler, T.J., Rudy, J.W., 2007. The hippocampal indexing theory and episodic memory: Updating the index. Hippocampus 17 (12), 1158–1169. https://doi.org/10.1002/hipo.20350.

Tulving, E., Kapur, S., Craik, F.I., Moscovitch, M., Houle, S., 1994. Hemispheric encoding/retrieval asymmetry in episodic memory: positron emission tomography findings. PNAS 91 (6), 2016–2020. https://doi.org/10.1073/pnas.91.6.2016.

van de Nieuwenhuijzen, M.E., Backus, A.R., Bahramisharif, A., Doeller, C.F., Jensen, O., van Gerven, M.A.J., 2013. MEG-based decoding of the spatiotemporal dynamics of visual category perception. Neuroimage 83, 1063–1073. https://doi.org/10.1016/j.neuroimage.2013.07.075.

Virtanen, P., Gommers, R., Oliphant, T.E., Haberland, M., Reddy, T., Cournapeau, D., Burovski, E., Peterson, P., Weckesser, W., Bright, J., van der Walt, S.J., Brett, M., Wilson, J., Millman, K.J., Mayorov, N., Nelson, A.R.J., Jones, E., Kern, R., Larson, E., Vázquez-Baeza, Y., 2020. SciPy 1.0: fundamental algorithms for scientific computing in Python. Nat. Methods 17 (3), 261–272. https://doi.org/10.1038/s41592-019-0686-2.

Vogelsang, D.A., Bonnici, H.M., Bergström, Z.M., Ranganath, C., Simons, J.S., 2016. Goal-directed mechanisms that constrain retrieval predict subsequent memory for new “foil” information. Neuropsychologia 89, 356–363. https://doi.org/10.1016/j.neuropsychologia.2016.07.016.

Waddill, P.J., McDaniel, M.A., 1998. Distinctiveness effects in recall. Memory Cognit. 26 (1), 108–120. https://doi.org/10.3758/BF03211374.

Wagner, A.D., Poldrack, R.A., Eldridge, L.L., Desmond, J.E., Glover, G.H., Gabrieli, E., J. D., 1998. Material-specific lateralization of prefrontal activation during episodic encoding and retrieval. Neuroreport 9 (16), 3711–3717. https://doi.org/10.1097/00001756-199811160-00026.

Wang, C., Xiong, S., Hu, X., Yao, L., Zhang, J., 2012. Combining features from ERP components in single-trial EEG for discriminating four-category visual objects. J. Neural Eng. 9 (5), 056013. https://doi.org/10.1088/1741-2560/9/5/056013.

Watanabe, S., Kakigi, R., Puce, A., 2003. The spatiotemporal dynamics of the face inversion effect: A magneto- and electro-encephalographic study. Neuroscience 116 (3), 879–895. https://doi.org/10.1016/S0306-4522(02)00752-2.

Wolk, D.A., Schacter, D.L., Lygizos, M., Sen, N.M., Holcomb, P.J., Daffner, K.R., Budson, A.E., 2006. ERP correlates of recognition memory: Effects of retention interval and false alarms. Brain Res. 1096 (1), 148–162. https://doi.org/10.1016/j.brainres.2006.04.050.

Wolk, D.A., Sen, N.M., Chong, H., Riis, J.L., McGinnis, S.M., Holcomb, P.J., Daffner, K.R., 2009. ERP correlates of item recognition memory: Effects of age and performance. Brain Res. 1250, 218–231. https://doi.org/10.1016/j.brainres.2008.11.014.

Xie, S., Hoehl, S., Moeskops, M., Kayhan, E., Kliesch, C., Turtleton, B., Köster, M., Cichy, R.M., 2022. Visual category representations in the infant brain. Curr. Biol. 32 (24), 5422–5432.e6. https://doi.org/10.1016/j.cub.2022.11.016.

Yassa, M.A., Stark, C.E.L., 2011. Pattern separation in the hippocampus. Trends Neurosci. 34 (10), 515–525. https://doi.org/10.1016/j.tins.2011.06.006.

Yick, Y.Y., Buratto, L.G., Schaefer, A., 2016. Variations in prestimulus neural activity predict the emotion-enhanced memory effect. Neuroreport 27 (11), 864–868. https://doi.org/10.1097/WNR.0000000000000628.

Yildirim-Keles, F.Z., Stacchi, L., Caldara, R., 2025. Cross-validating the electrophysiological markers of early face categorization. ENEURO.0317-24.2024 Eneuro 12 (1). https://doi.org/10.1523/ENEURO.0317-24.2024.

Yonelinas, A.P., 2002. The nature of recollection and familiarity: A review of 30 years of research. J. Mem. Lang. 46 (3), 441–517. https://doi.org/10.1006/jmla.2002.2864.